

# UC Berkeley

## UC Berkeley Previously Published Works

### Title

Neurometabolic coupling between neural activity, glucose, and lactate in activated visual cortex

### Permalink

<https://escholarship.org/uc/item/2pw8k804>

### Journal

Journal of Neurochemistry, 135(4)

### ISSN

0022-3042

### Authors

Li, Baowang  
Freeman, Ralph D

### Publication Date

2015-11-01

### DOI

10.1111/jnc.13143

Peer reviewed



# HHS Public Access

Author manuscript

*J Neurochem.* Author manuscript; available in PMC 2016 November 01.

Published in final edited form as:

*J Neurochem.* 2015 November ; 135(4): 742–754. doi:10.1111/jnc.13143.

## Neurometabolic coupling between neural activity, glucose and lactate in activated visual cortex

Baowang Li and Ralph D. Freeman\*

Group in Vision Science, School of Optometry, Helen Wills Neuroscience Institute, University of California, Berkeley, CA 94720-2020

### Abstract

Neural activity is closely coupled with energy metabolism but details of the association remain to be identified. One basic area involves the relationships between neural activity and the main supportive substrates of glucose and lactate. This is of fundamental significance for the interpretation of non-invasive neural imaging. Here, we use microelectrodes with high spatial and temporal resolution to determine simultaneous co-localized changes in glucose, lactate and neural activity during visual activation of the cerebral cortex in the cat. Tissue glucose and lactate concentration levels are measured with electrochemical microelectrodes while neural spiking activity and local field potentials are sampled by a microelectrode. These measurements are performed simultaneously while neurons are activated by visual stimuli of different contrast levels, orientations, and sizes. We find immediate decreases in tissue glucose concentration and simultaneous increases in lactate during neural activation. Both glucose and lactate signals return to their baseline levels instantly as neurons cease firing. No sustained changes or initial dips in glucose or lactate signals are elicited by visual stimulation. However, co-localized measurements of cerebral blood flow (CBF) and neural activity demonstrate a clear delay in the CBF signal such that it does not correlate temporally with the neural response. These results provide direct real-time evidence regarding the coupling between co-localized energy metabolism and neural activity during physiological stimulation. They are also relevant to a current question regarding the role of lactate in energy metabolism in the brain during neural activation.

### Keywords

glucose; lactate; metabolism; neural; visual cortex

### Introduction

Glucose is traditionally considered to be the main substrate for neuronal energy metabolism in the brain. Lactate production in the brain has been considered to be a waste product that

---

\*Correspondence to: Ralph D. Freeman, 360 Minor Hall, University of California at Berkeley, Berkeley, CA 94720-2020, USA, Tel & Fax: 510-642-6341, rfreeman@berkeley.edu.

#### Author contributions

B. L. and R.D.F designed the study, conducted the experiments, and wrote the manuscript.

#### Competing financial interests

The authors declare no competing financial interests.

results from inadequate oxygen delivery or a mismatch between glycolytic and oxidative rates (Siesjo 1978). However, the classic role of lactate has been challenged by proposals that it is also an energy source that neurons use as a glial-released substrate (Bouzier-Sore et al. 2003, Larrabee 1995, Magistretti & Pellerin 1999, Magistretti et al. 1999, Pellerin & Magistretti 1994, Pellerin et al. 1998, Poitry-Yamate et al. 1995). This notion is derived from *in vitro* experiments with cultured cells, but a few *in vivo* studies suggest lactate as a preferred or supplementary fuel for neurons (Boumezbeur et al. 2010, Sampol et al. 2013, Wyss et al. 2011). The methods used for the *in vivo* studies include functional magnetic resonance spectroscopy, fluoro-deoxyglucose positron emission tomography, and other non-invasive techniques (Caesar et al. 2008, Fellows et al. 1993, Gjedde & Marrett 2001, Lowry et al. 1998, Mangia et al. 2007, Smith et al. 2003, Vlassenko et al. 2006, Wyss et al. 2011). Note that these methods have coarse temporal or spatial resolution or both and cannot capture the rapid alterations in metabolite concentration that occur in localized brain regions.

On the other hand, electrochemical techniques, which have been used for measuring changes in neurotransmitters and metabolites in the brain, provide high temporal and/or spatial resolution compared to the above techniques (Hu et al. 1994, Hu & Wilson 1997b, Hu & Wilson 1997a, Wilson et al. 1992). In studies of rat cortex, it has been reported that repetitive electric stimulation elicited enhanced extracellular lactate and reduced glucose levels with larger initial dips for lactate compared to those for glucose (Hu & Wilson 1997b). (These findings were interpreted by the authors as evidence that activated neurons prefer lactate over glucose. However, these results were obtained by use of a non-physiological stimulus, and neural activity was not measured. In the current study, we use electrochemical glucose and lactate sensors and a neural microelectrode to measure simultaneously changes in extracellular glucose and lactate signals and coordinated neural responses to visual stimuli. Our approach, monitoring an active portion of cerebral cortex, provides a realistic and relatively complete physiological profile of the components we are addressing. We find strong and rapid transient changes in lactate and glucose signals during neuronal firing. There are no sustained responses or initial transient dips for either lactate or glucose signals.

## Materials and methods

### Physiological procedures

All procedures were conducted in accordance with the guidelines approved by NIH and by the Animal Care and Use Committee at the University of California, Berkeley. We studied anesthetized cats prepared as follows. Each animal was initially anesthetized with 3% isoflurane which was reduced to 2–2.5% following stabilization as assessed by loss of withdrawal reflex in response to toe pinch. Catheters were inserted into femoral veins in all four legs and a tracheal cannula was positioned. Isoflurane was discontinued and anesthesia was continued with intravenous infusion of propofol (15–20 mg/(kg·hr)) and fentanyl (10 µg/(kg·hr)). The animal was artificially ventilated with a mixture of 25% O<sub>2</sub> and 75% N<sub>2</sub>O. Expired CO<sub>2</sub> was maintained at 32–38 mmHg. Rectal temperature was monitored and maintained at 38 °C by a feedback-controlled heating blanket. A craniotomy was made above the central representation of the visual field in the striate cortex (Horsley-Clark

coordinates P4L2) and the dura was dissected. After surgical procedures were finished, infusion rates of fentanyl and propofol were gradually reduced to 4–6  $\mu\text{g}/(\text{kg}\cdot\text{hr})$  and 6–10  $\text{mg}/(\text{kg}\cdot\text{hr})$ , respectively, as determined for each animal. A neuromuscular blocking agent, gallamine triethiodide, was delivered to prevent eye movements (10  $\text{mg}/(\text{kg}\cdot\text{hr})$ ). Lactated Ringer solution with 5% dextrose was infused at a rate of 4  $\text{ml}/(\text{kg}\cdot\text{hr})$  to prevent dehydration. Contact lenses (+2D) with artificial pupils of 4 mm were placed on both corneas. EEG, ECG, and intra-tracheal pressure were monitored throughout the experiment. An overdose of Euthasol was given to the animal at the end of each experiment.

### Visual stimulation

Visual stimuli consisted of drifting sinusoidal gratings that were presented on two CRT monitors for left and right eyes, respectively. The refresh rate of the monitors was 85 Hz. The mean luminance was 45  $\text{cd}/\text{m}^2$ . Stimuli were presented to the dominant eye while the non-dominant eye viewed a blank gray isoluminant screen (45  $\text{cd}/\text{m}^2$ ). For each recording site, optimal stimulus parameters (orientation, spatial frequency, temporal frequency and size) were obtained quantitatively from tuning functions. To examine response characteristics of neural and metabolic responses, different stimulus contrasts (10%, 20%, 40%, and 80%), orientations (preferred and orthogonal), sizes (optimal and full-field), and durations (1, 2 and 30 s) were included in each experiment. Eight different inter-stimulus intervals (30–44 s) were varied randomly between stimulus conditions.

### Glucose and lactate electrodes

Glucose and lactate electrodes (Pinnacle Technology, 7005-Glucose-C and 7005-Lactate-C, Lawrence, KS) were used as in previous studies (Hu & Wilson 1997b, Wilson et al. 1992). In brief, the electrode is formed by a Teflon-coated Pt-Ir wire, which is wrapped concentrically with a AgCl reference electrode. At the tip of the composite electrode, a 1 mm section is exposed to form the sensing cavity. The tip is coated with glucose or lactate oxidase and a series of membranes in order to increase selectivity and specificity of the sensors. Detection of glucose and lactate signals is based on enzymes. When the analyte of interest (glucose or lactate) comes into contact with the enzyme, the enzyme catalytically processes the analyte to produce  $\text{H}_2\text{O}_2$ , which is directly proportional to the concentration of the analyte and is recorded with a Pt-Ir electrode as an oxidation current (typically in nanoamps (nA)). The inner membrane is composed of cellulose acetate and nafion, which are negatively charged and inhibit electroactive elements such as ascorbate and urate (Hu et al. 1994). Outside the inner membrane is an enzyme layer, which is covered by an outer layer based on a proprietary formulation of biocompatible polyurethane. This arrangement serves to reduce the flux of metabolites, protect the enzyme from biological fluid, and maintain the required peroxide.

Prior to physiological data collection in the visual cortex, each biosensor was calibrated *in vitro* to verify proper selectivity and sensitivity by assessing responses to glucose and lactate. All sensors responded to glucose or lactate linearly in 0.1M phosphate-buffered saline (PBS, pH 7.4). Once calibrated, the combined sensors (a glucose sensor, a lactate sensor, and a tungsten electrode) were advanced by a hand-controlled digital micromanipulator into the visual cortex. After recordings from a penetration, electrodes

were removed and recalibrated to verify that sensitivity to glucose and lactate was consistent with previous data implying that measurements were stable throughout the prolonged recording. A reduction of sensitivity between the original calibrations and post-experiment recalibrations was generally observed (Hu et al. 1994), and the linear component of the decay was taken into account in data analysis as follows. Differences in sensitivity between original and post-experiment calibrations were temporally integrated to obtain a sensitivity reduction slope. Sensitivity of a biosensor at a given time was estimated based on original calibration and slope, which assumes that decay is a temporally linear process.

### **Simultaneous measurements of neural, glucose and lactate signals**

Neural activity was recorded with an epoxy coated tungsten microelectrode (A-M systems, 5M $\Omega$ ). Neural signals were amplified and filtered to generate extracellular multiple unit activity (MUA, 0.25–8KHz) and LFP (0.7–170 Hz). Glucose and lactate signals were recorded with two separate biosensors. The biosensors were connected to a potentiostat in which the bio-signals were amplified and readings of the current were fed to a computer for data recording. The tip size of each biosensor is ~200  $\mu\text{m}$  in diameter. The two sensors were housed in a double-barrel guide cannula, which was controlled and advanced via a micromanipulator. The distance between the tips of the two biosensors is ~250  $\mu\text{m}$ . The tungsten neural electrode was positioned between the two biosensors and fixed by epoxy onto the guide cannula. The sampling rate for glucose and lactate signals was 10 Hz, and the sampling rate for neural spiking activity and LFP were 25 kHz and 500 Hz respectively. Time-dependent frequency analysis was applied to the LFP signal. The 60 Hz line noise and 85 Hz monitor refresh rate were removed by applying a Matlab function of noise removal (rmlinesc.m, Chronux toolbox, <http://chronux.org/>). LFP spectrograms were then calculated on a 500-ms window and a 50-ms step size with a multi-taper spectral estimation (Thomson 1982). The power of baseline activity in the pre-stimulus period (10s) and for long and short stimulus durations (30 s and 1–2 s, respectively), was subtracted from the LFP spectrograms. The power at each frequency and time bin was then normalized by the average power for that frequency in the baseline. For each recording site, modulation of LFP power was averaged over trials.

### **Simultaneous measurements of neural and cerebral blood flow (CBF) signals**

CBF signals were recorded with a fine laser Doppler flow (LDF) needle probe (MP4S, Moor Instruments, UK). The external diameter of the LDF probe is 460  $\mu\text{m}$ . Neural activity was recorded with a tungsten microelectrode (A-M systems, 5M  $\Omega$ ), which was attached to the LDF probe by epoxy. The combined sensors were advanced by a digital micromanipulator into visual cortex. The LDF probe was connected to a monitor (Moorlab server, Moor Instruments, UK). The LDF signal was amplified by the monitor and then A/D converted and sampled at 10 Hz. The LDF device was calibrated with a standard calibration solution provided by the manufacturer prior to data recording.

### **Data analysis**

Recorded signals were analyzed by Matlab (MathWorks). Slow-frequency oscillations were observed for glucose, lactate, and especially LDF signals for some recording sites. To enhance the signal to noise ratio, multiple trials (8–48) were obtained for each stimulus

condition. To compare temporal coupling between neural, glucose and lactate responses to visual stimulation, spiking activity was resampled at 10Hz instead of 25KHz, to allow comparisons with glucose and lactate signals. A response is considered to be significant if it shows statistically significant ( $p < 0.05$ , t test) change compared to the baseline signal, which is determined as the signal level 10s prior to stimulus onset. To examine differences between responses to different stimulus conditions, statistical significance is assessed by pairwise comparisons of signals (Wilcoxon sign rank tests). Values are expressed as means  $\pm$  s.e.m.

## Results

We studied responses from 31 recording sites in visual cortex from 9 mature cats (aged 5–10 months; 2.5–4.0 Kg). Of the total, 25 sites were tested with visual stimuli of different contrast levels and 6 were examined with stimuli of different orientations or sizes.

### Co-localized glucose, lactate, and neural activity to visual stimuli of different contrasts

Simultaneous measurements were made, in co-localized cortical regions, of glucose, lactate, and neural responses to visual stimuli. Four contrast levels (10%, 20%, 40% and 80%) were used to provide different levels of neural and metabolic responses as illustrated in Figure 1. Stimuli at all contrast levels elicited vigorous increases in spiking activity (left column, Fig. 1a) and lactate concentration (left column, Fig. 1d) with simultaneous decreases in glucose (left column, Fig. 1c) for a representative recording site. No observable response is elicited for the LFP signal (left column, Fig. 1b). To visualize detailed temporal profiles of the changes in the three measurements, data within the two black vertical dashed lines (left column, Fig. 1a–d, 20% stimulus contrast) are zoomed in on (expanded) and illustrated in the middle column (Fig. 1a–d). Similarly, data within the two red vertical dashed lines (middle column, Fig. 1a–d) are zoomed in on again and shown on the right (right column, Fig. 1a–d). This recording site exhibits simple-cell like spiking activity that is modulated in synchrony with the temporal frequency (2 Hz) of stimulation (Movshon et al. 1978). Glucose and lactate signals also exhibit modulated responses that are generally in synchrony with the spiking activity. When neurons are activated by the visual stimulus, glucose concentrations decrease rapidly while lactate levels immediately increase. During silent periods of spiking activity, glucose and lactate quickly return to baseline levels. This pattern of spiking, glucose, and lactate responses repeats until the visual stimulus is removed at which time, all three measurements return to baseline levels. These coupled changes in spiking activity, glucose, and lactate are present for all contrast levels across all trials. The local field potentials (LFPs), as illustrated by modulated power (Fig. 1b, middle and right columns), however, do not exhibit significant responses to visual stimulation. The lack of LFP responses is consistently observed for visual stimuli at all contrast levels. This is possibly due to the location of the neural electrode tip for this recording site. LFPs are reported to vary significantly in gamma-band power across cortical layers with minimum values in layer 4C $\beta$ , 5 and 6 of V1 (Xing et al. 2012). The depth of this recording site is 4.03 mm (H-C coordinates P4L2), which may be located in one of the above layers with minimum gamma-power of LFP.

To assess the coupling between the three measurements, we calculate time differences between peaks in spiking activity (LFP is not included in the time analysis because it is too weak at this recording site), dips in glucose, and peaks in lactate response. A data point is defined as a peak (or dip) if it is bigger (or smaller) than two data points on its immediate left and another two data points on the adjacent right. As shown in Fig. 1e–g, time differences are 0 within the experimental temporal resolution (100 ms, which is the reverse of the 10-Hz sampling rate) for nearly all peaks and dips, which demonstrate that events occur simultaneously and changes in the three measurements are tightly associated. We believe these data to be the first to show close coupling between neural, glucose, and lactate signals in an in vivo preparation. Average responses over time across 16 trials for the same recording site are shown in Fig. 2. Neural responses include low levels of spontaneous spiking as shown in the histograms 10 s prior to stimulus onset (Fig. 2a). Glucose and lactate responses (Fig. 2b, c) are presented as percentages of change relative to the baseline spontaneous levels, which are subtracted from respective signals. Percent changes in signals are computed by averaging responses across trials. Baselines of signals are taken to be signal levels 10s prior to stimulus onset. Responses are normalized by baseline levels and presented as percentages of signal change. The data clearly demonstrate co-localized activity-dependent changes in glucose and lactate levels. Glucose and lactate concentrations vary in opposite directions immediately following neural firing and both signals return to baseline levels as neurons cease activity. In previous studies, sustained increased extracellular lactate and decreased glucose levels have been reported during stimulation (Caesar et al. 2008, Mangia et al. 2007, Prichard et al. 1991, Sampol et al. 2013, Smith et al. 2003, Wyss et al. 2011). However, low temporal resolution in this previous work did not permit relevant detailed temporal profiles of changes in both glucose and lactate signals. To demonstrate that our current results have similar overall profiles to previous data, we reduce the temporal resolution of our data from 10 Hz (Fig. 2a–c) to 2 Hz by averaging responses of every 5 data points along the horizontal axis and re-plot the data for neural (Fig. 2d), glucose (Fig. 2e) and lactate (Fig. 2f) responses, respectively. As predicted, all measurements demonstrate sustained changes during visual stimulation consistent with those of previous reports. To elucidate the relationship between metabolic responses and the underlying neural activity, we obtain mean values over the entire stimulus-presentation duration for four stimulus-contrast levels for neural, glucose, and lactate responses (Fig. 2g). Changes in glucose and lactate signals clearly increase together with stimulus contrast, and this increase is directly attributable to analogously increased neural activity (Fig. 2h).

In a previous study with biosensors (Hu & Wilson 1997b), glucose and lactate responses were elicited only by long-duration electrical stimulation (5s) whereas shorter-duration stimuli caused no observable alteration in the dentate gyrus of the hippocampus in rats. This result is at odds with our observation that both glucose and lactate change instantly following the onset of visual stimulation. To extend our finding, we recorded neural, glucose and lactate responses to 2-s visual stimuli at 10%, 20%, 40% and 80% contrast levels for 3 recording sites. Figure 3 illustrates responses of an example recording site (8 repetitions). The short-duration stimulation elicited increases in spiking activity (Fig. 3a), gamma-power LFPs (Fig. 3c), and lactate signal (Fig. 3g) together with decreases in glucose signal (Fig. 3e). Average responses across trials for these four measurements are shown in Fig. 3b, d, f,

and h, and they appear to be modulated at the temporal frequency (2Hz) of the visual stimuli. Both glucose and lactate signals return to baseline levels immediately during silent phases of neural activity. They change again during neural firing phases, and finally go back to baseline levels at the end of visual stimulation. Normalized mean responses of neural, glucose and lactate responses across stimulus duration and trials are compared in Fig. 3i. For visualization, changes in glucose signal are illustrated with absolute values. Response times for the four peaks (Fig. 3b, d, and h) and the four dips (Fig. 3f) across the 2-s stimulus duration are averaged across all contrast levels and shown in Fig. 3j. For the tested contrasts, neural, glucose and lactate responses are clearly closely coupled.

The coupling for activity-induced changes in neuronal, glucose and lactate signals is consistent across a population of recording sites ( $n = 25$ ). Peaks (MUA and lactate) or dips (glucose) during visual stimuli of different contrast levels are obtained from multiple-trial (8–48) averaged responses for each recording site. In total, visual stimuli of 10%, 20%, 40% and 80% contrast levels elicit 1317, 1322, 1316, and 1320 peaks in spiking activity, 1067, 1130, 1184, and 1211 dips in glucose response, and 1296, 1308, 1310 and 1317 peaks in lactate response from all recording sites (Fig. 4a). This represents 81.0%, 85.4%, 90.0%, and 91.7% for dips in glucose and 98.4%, 98.9%, 99.5%, and 99.8% for peaks in lactate with respect to the numbers of peaks in spiking activity for the four contrast levels (Fig. 4b). Thus, glucose dips and lactate peaks are observed for nearly all peaks in neural activity. Note that lactate peaks are more likely to be observed than glucose dips ( $p = 0$ , Z test). The time difference between glucose dips and corresponding spiking peaks is  $5.06 \pm 3.21 \times 10^{-4}$  s ( $n=4543$ , Fig. 4c). Similarly, the time difference between lactate and spiking peaks is  $4.58 \pm 2.33 \times 10^{-4}$  s ( $n=5181$ , Fig. 4d) for responses to visual stimuli at the four contrast levels. Taken together, the events occur simultaneously (within the experimental temporal resolution) for 81.41% (3741 out of 4595) of the pairs of glucose dips and spiking peaks, and for 97.15% (5084 out of 5233) of the pairs of lactate and spiking peaks. Clearly, activation induced changes in neural, glucose, and lactate signals appear to occur simultaneously during visual stimulation.

Neurons in striate cortex are selective to visual stimulus parameters, including orientation, direction, spatial and temporal frequencies, position and size. Here, we use visual stimuli at two orientations (preferred and orthogonal) within the classical receptive field (RF) to examine if glucose and lactate signals possess the same preferences for stimulus orientation as neural response. As shown in Fig. 5 for a representative recording site (8 repetitions), the preferred orientation, which is pre-determined by an orientation tuning function, elicits vigorous MUA and LFP (Fig. 5a, b, left column), and concurrent changes in opposite directions for glucose (Fig. 5c, left column) and lactate (Fig. 5d, left column) signals. The orthogonal orientation,  $90^\circ$  from the preferred, elicits no responses (Fig. 5a–d, right column). We also examine the coupling between neural activity, glucose and lactate responses to visual stimuli of different sizes (optimal and full- field sizes). The optimal size consists of the stimulus dimensions that elicit maximum spiking activity while the full-field size represents a visual stimulus covering the entire screen of the monitor. As shown in Fig. 6 for an example recording site (32 repetitions), the stimulus at optimal size ( $2^\circ$  in diameter) produces stronger MUA (Fig. 6a, left column) and LFP (Fig. 6b, left column) responses, negative changes in glucose signal (Fig. 6c, left column), and positive changes in lactate



signal (Fig. 6d, left column) compared to those for the full-field stimulus (Fig. 6a–d, right column). Similar results were observed from an additional four recording sites (two for orientation, and two for size). These findings demonstrate that neural, glucose and lactate signals have the same selectivity for size of visual stimuli, which is again consistent with close coupling between these measurements during use of different contrast levels.

Glucose consumption has been shown to be proportional to changes in cerebral blood flow (CBF) (Fox & Raichle 1986, Fox et al. 1988). To determine if the response profiles of glucose and lactate signals we report here are accounted for by changes in CBF, we have made simultaneous recordings of CBF and neural responses to visual stimuli as shown for a representative recording site (Fig. 7). The MUA and LFP in this case are modulated in synchrony with the temporal frequency of stimulation (Fig. 7a, b). However, the CBF response (Fig. 7c) is clearly different from the modulated responses of glucose and lactate signals that we have shown in this study. Here, the CBF response consists of a sustained high level with minor fluctuations during the response. Furthermore, spiking activity, LFP and CBF signals reach peaks at 0.96 s, 0.9 s and 5.34 s, respectively. Therefore, the CBF signal clearly lags behind and does not temporally correlate with the neural response.

## Discussion

By using high spatial and temporal resolution micro-sensors, we have obtained direct evidence on co-localized dynamic changes in extracellular glucose and lactate signals and their related neural activity from stimulation of visual cortex. Glucose and lactate responses are transient and closely follow changes in neural activity. Decreased glucose and elevated lactate are not sustained, and levels of both elements are restored to baseline instantly as neurons stop firing. To our knowledge, this is the first study to demonstrate transient changes in extracellular glucose and lactate signals that are dynamically coupled with neural activity in an intact nervous system. We have obtained both multiple unit activity (MUA) and LFP data in addition to measurements of glucose and lactate tissue concentrations. We should note that there is considerable variability in the LFP data which for some of our results are relatively weak. It is possible that this may be due to equipment issues but we did multiple control measurements as described in Methods and did not find any source for variability of signal strength.

Enzyme-based lactate micro-sensors have been used previously to measure real time extracellular lactate concentration variations due to electrical stimulation of the hippocampus of anesthetized rats (Hu & Wilson 1997b). In this latter study, following repetitive stimulation, extracellular lactate was increased twofold to a sustained level which stayed elevated during 2-min rest intervals. This is inconsistent with our current findings and other work in which lactate concentration returns to baseline levels after physiological stimulation (Caesar et al. 2008, Mangia et al. 2007, Prichard et al. 1991, Sampol et al. 2013). In addition, neural activity was not measured (Hu & Wilson 1997b). Repetitive electrical stimulation can cause seizure-like activity (Dienel 2012), and the sustained elevation of lactate could be due to excessive electrical stimulation which may cause firing of large groups of neurons. This possibility is emphasized for the long-duration stimuli required in their experiments. No observable changes were found in glucose and lactate concentrations

for stimulus durations shorter than 5 s (Hu & Wilson 1997b). As we show here, glucose and lactate exhibit substantial responses from stimulation by visual stimuli of much shorter durations (1–2 s, Fig. 3 and Fig. 6). Thus, long-duration stimulation is not required to elicit the substantial glucose and lactate responses detected by biosensors. It is possible that a long-duration (>5 s) electric stimulus was needed to elicit local seizure activity in the previous experiments (Hu & Wilson 1997b). Alternatively, the animals used in their experiments might have been in a hypoxic condition. Lactate level is reported to rise steeply to very high levels when animals are hypoxic. (Jones et al. 2000, Ros et al. 2002, Schurr et al. 1997, Yanai et al. 1997). However, it should be noted that lactate levels are the net result of inputs and outputs. These include lactate influx and efflux across the blood brain barrier and across the membranes of brain cells, lactate production from glucose and glycogen, lactate metabolism within brain cells, diffusion to and from the sensors, and changes in the size of extracellular space. All these factors may contribute to the change of extracellular lactate levels.

In addition to sustained high concentrations of lactate, observations have also been made of a small initial dip in extracellular lactate concentration after electric stimulation (Hu & Wilson 1997b). In our current study, we do not observe an initial dip in the lactate signal. We assume that the initial dip in the previous work may be ascribed to the sustained high level of lactate. Previous *in vitro* studies have found that glucose utilization was substantially suppressed while lactate metabolism was increased at high lactate concentrations (Itoh et al. 2003, Larrabee 1995). It is possible that the initial dip elicited by electrical stimulation (Hu & Wilson 1997b) was due to an increased lactate metabolism as its concentration was elevated. In addition, the amplitude of the initial dip of the lactate signal increased with lactate concentration during repetitive electrical stimulation (Hu & Wilson 1997b). This is consistent with *in vitro* observations that the suppression of glucose utilization and lactate metabolism increases with lactate concentration for both neurons and astrocytes (Itoh et al. 2003, Larrabee 1995).

As we show here in Fig. 4, lactate peaks are more likely to be observed than glucose dips during peaks in neural response, which suggests that other processes in addition to glycolysis may contribute to the production of lactate. In the brain, only astrocytes are able to store glucose as glycogen. The breakdown of glycogen in astrocytes (glycogenolysis) is low during resting conditions, but it can be greatly enhanced when energy demand is high during brain activation (Brown et al. 2004, Newman et al. 2011, Swanson et al. 1992). It is possible that glucose phosphate produced from glycogenolysis in astrocytes may account for fewer glucose dips (compared to lactate peaks) in our observations. We also find larger percent increases in lactate than decreases in glucose during neural activation. Glycolysis and glycogenolysis may both contribute to the higher relative changes in lactate. In anaerobic glycolysis, if two units of lactate are generated from one unit of glucose, the change in total lactate should be double that of glucose assuming the basal concentrations of these two substrates are the same (Dienel & Cruz 2008). Because glucose concentration in a resting brain is generally higher than that of lactate, as shown in the current study and in previous work (Dienel 2012), the percentage of change in lactate can be even larger. Additionally, glycogenolysis in astrocytes may further increase the difference between relative changes in glucose and lactate.

Normal brain functions depend on continuous delivery of glucose and oxygen by the blood. The delivery of glucose to the brain across the blood–brain barrier is mediated by glucose transporter proteins. The steady-state brain-to-plasma ratio for glucose is 0.2–0.3 in rats (Dienel et al. 1991), and there is close coupling between glucose delivery and local CBF (Sokoloff 1992). However, our results demonstrate that there is a clear dissociation between activity-induced changes in glucose and CBF signals. Glucose rapidly decreases with neural activity and returns to baseline level immediately as neurons stop firing. The CBF response, however, remains at a sustained high level during visual stimulation. The delayed onset and extended time course of the CBF response may reflect involvement of mechanisms with long time constants (Mathiesen et al. 2000).

Glucose is traditionally considered the sole substrate for neuronal energy metabolism in the brain while lactate has long been viewed as a waste product (Siesjo 1978). In the past two decades, this notion has been challenged by the astrocyte-neuron lactate shuttle (ANLS) hypothesis in which glucose is taken by glial cells to produce lactate to fuel neurons (Pellerin & Magistretti 1994). However, direct evidence from an intact brain is needed to test the ANLS hypothesis. In a previous *in vivo* study (Hu & Wilson 1997b), a larger initial decrease in extracellular lactate was elicited than in extracellular glucose when a sustained level of lactate concentration had been previously elevated by repetitive electrical stimulation. These previous findings appear to be consistent with the ANLS hypothesis. However, electrical stimulation of cerebral neuronal pathways is an uncommon condition, since in an intact brain, it is unlikely that all neurons of a pathway are synchronized. Thus, caution is needed when interpreting these results. In the current study, by using physiological stimulation, we find transient decreases in extracellular glucose concentration and transient increases in extracellular lactate levels, and changes in both signals return to baseline levels immediately as neurons cease firing. Neither sustained elevated lactate levels nor initial dips in lactate were observed in our experiments. Although needle-shaped biosensors have high temporal resolution (the 90% maximum response time is 1.3 s (Hu et al. 1994)), they cannot detect instant co-localized changes in glucose and lactate signals that are likely to be closely coupled with individual spiking events (~1 ms). This limitation means that it is not possible to determine if produced lactate is locally consumed or released from activated areas to the blood. If consumed, it is also not possible to specify if the mechanism is related to local neurons or glial cells. In addition, it cannot be determined if decreases in glucose signals are associated with anaerobic glycolysis in neurons or in glial cells.

In conclusion, with use of simultaneous co-localized measurements of extracellular glucose, lactate, and neural responses to physiological stimuli, we observe transient changes in glucose and lactate signals that are closely coupled with neural activity. No initial dips or sustained changes are shown in glucose or lactate signals. Our results are not directly applicable to the previously considered astrocyte-neuron lactate shuttle since we cannot determine which cell types consume glucose and generate lactate. However, our approach provides real time high-resolution evidence of biochemical and physiological components during active neural processing.

## Acknowledgments

This work was supported by National Eye Institute Research Grant EY01175. We thank T. Kim for help with experiments.

## Abbreviations

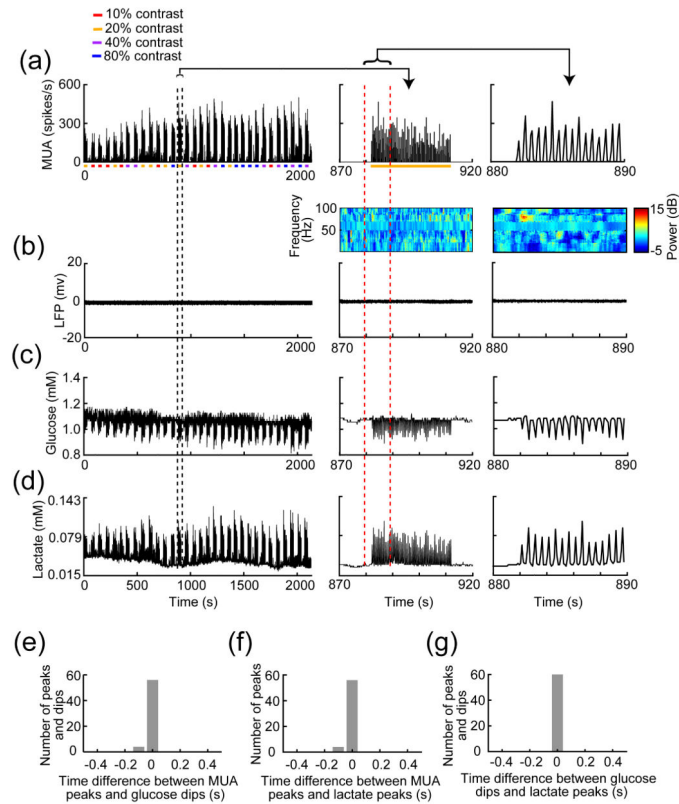
<b>mg</b>	milligram
<b>kg</b>	kilogram
<b>hr</b>	hour
<b>µg</b>	microgram
<b>SEM</b>	standard error of the mean
<b>ms</b>	milliseconds
<b>dura</b>	duramater
<b>Ir</b>	iridium
<b>AgCl</b>	silver chloride
<b>nA</b>	nanoamps
<b>KHz</b>	kilohertz

## References

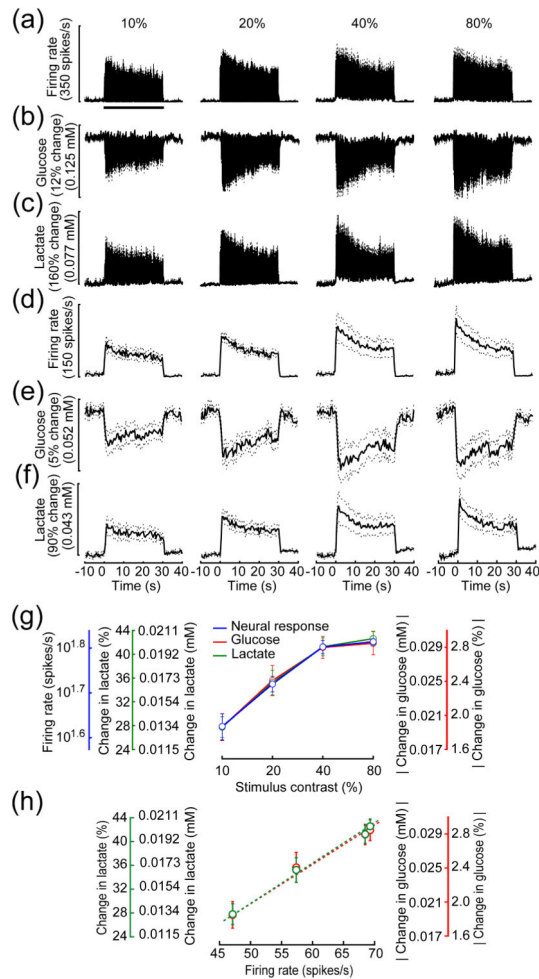
- Boumezbeur F, Petersen KF, Cline GW, Mason GF, Behar KL, Shulman GI, Rothman DL. The contribution of blood lactate to brain energy metabolism in humans measured by dynamic <sup>13</sup>C nuclear magnetic resonance spectroscopy. *The Journal of Neuroscience*. 2010; 30:13983–13991. [PubMed: 20962220]
- Bouzier-Sore AK, Voisin P, Canioni P, Magistretti PJ, Pellerin L. Lactate is a preferential oxidative energy substrate over glucose for neurons in culture. *Journal of Cerebral Blood Flow & Metabolism*. 2003; 23:1298–1306. [PubMed: 14600437]
- Brown AM, Baltan Tekkok S, Ransom BR. Energy transfer from astrocytes to axons: the role of CNS glycogen. *Neurochem Int*. 2004; 45:529–536. [PubMed: 15186919]
- Caesar K, Hashemi P, Douhou A, Bonvento G, Boutelle MG, Walls AB, Lauritzen M. Glutamate receptor-dependent increments in lactate, glucose and oxygen metabolism evoked in rat cerebellum in vivo. *The Journal of Physiology*. 2008; 586:1337–1349. [PubMed: 18187464]
- Dienel GA. Brain lactate metabolism: the discoveries and the controversies. *Journal of Cerebral Blood Flow & Metabolism*. 2012; 32:1107–1138. [PubMed: 22186669]
- Dienel GA, Cruz NF. Imaging brain activation: simple pictures of complex biology. *Ann N Y Acad Sci*. 2008; 1147:139–170. [PubMed: 19076439]
- Dienel GA, Cruz NF, Mori K, Holden JE, Sokoloff L. Direct measurement of the lambda of the lumped constant of the deoxyglucose method in rat brain: determination of lambda and lumped constant from tissue glucose concentration or equilibrium brain/plasma distribution ratio for methylglucose. *Journal of Cerebral Blood Flow & Metabolism*. 1991; 11:25–34. [PubMed: 1984002]
- Fellows LK, Boutelle MG, Fillenz M. Physiological stimulation increases nonoxidative glucose metabolism in the brain of the freely moving rat. *Journal of Neurochemistry*. 1993; 60:1258–1263. [PubMed: 8455025]

- Fox PT, Raichle ME. Focal physiological uncoupling of cerebral blood flow and oxidative metabolism during somatosensory stimulation in human subjects. *Proc Natl Acad Sci U S A*. 1986; 83:1140–1144. [PubMed: 3485282]
- Fox PT, Raichle ME, Mintun MA, Dence C. Nonoxidative glucose consumption during focal physiologic neural activity. *Science*. 1988; 241:462–464. [PubMed: 3260686]
- Gjedde A, Marrett S. Glycolysis in neurons, not astrocytes, delays oxidative metabolism of human visual cortex during sustained checkerboard stimulation in vivo. *Journal of Cerebral Blood Flow & Metabolism*. 2001; 21:1384–1392. [PubMed: 11740199]
- Hu Y, Mitchell KM, Albadily FN, Michaelis EK, Wilson GS. Direct measurement of glutamate release in the brain using a dual enzyme-based electrochemical sensor. *Brain Res*. 1994; 659:117–125. [PubMed: 7820652]
- Hu Y, Wilson GS. Rapid changes in local extracellular rat brain glucose observed with an in vivo glucose sensor. *J Neurochem*. 1997a; 68:1745–1752. [PubMed: 9084449]
- Hu Y, Wilson GS. A temporary local energy pool coupled to neuronal activity: fluctuations of extracellular lactate levels in rat brain monitored with rapid-response enzyme-based sensor. *Journal of Neurochemistry*. 1997b; 69:1484–1490. [PubMed: 9326277]
- Itoh Y, Esaki T, Shimoji K, Cook M, Law MJ, Kaufman E, Sokoloff L. Dichloroacetate effects on glucose and lactate oxidation by neurons and astroglia in vitro and on glucose utilization by brain in vivo. *Proc Natl Acad Sci U S A*. 2003; 100:4879–4884. [PubMed: 12668764]
- Jones DA, Ros J, Landolt H, Fillenz M, Boutelle MG. Dynamic changes in glucose and lactate in the cortex of the freely moving rat monitored using microdialysis. *J Neurochem*. 2000; 75:1703–1708. [PubMed: 10987853]
- Larrabee MG. Lactate metabolism and its effects on glucose metabolism in an excised neural tissue. *Journal of Neurochemistry*. 1995; 64:1734–1741. [PubMed: 7891102]
- Lowry JP, O'Neill RD, Boutelle MG, Fillenz M. Continuous monitoring of extracellular glucose concentrations in the striatum of freely moving rats with an implanted glucose biosensor. *Journal of Neurochemistry*. 1998; 70:391–396. [PubMed: 9422386]
- Magistretti PJ, Pellerin L. Astrocytes Couple Synaptic Activity to Glucose Utilization in the Brain. *News in Physiological Sciences*. 1999; 14:177–182. [PubMed: 11390847]
- Magistretti PJ, Pellerin L, Rothman DL, Shulman RG. Energy on demand. *Science*. 1999; 283:496–497. [PubMed: 9988650]
- Mangia S, Tkac I, Gruetter R, Van de Moortele PF, Maraviglia B, Ugurbil K. Sustained neuronal activation raises oxidative metabolism to a new steady-state level: evidence from 1H NMR spectroscopy in the human visual cortex. *Journal of Cerebral Blood Flow & Metabolism*. 2007; 27:1055–1063. [PubMed: 17033694]
- Mathiesen C, Caesar K, Lauritzen M. Temporal coupling between neuronal activity and blood flow in rat cerebellar cortex as indicated by field potential analysis. *J Physiol*. 2000; 523(Pt 1):235–246. [PubMed: 10673558]
- Movshon JA, Thompson ID, Tolhurst DJ. Spatial summation in the receptive fields of simple cells in the cat's striate cortex. *The Journal of Physiology*. 1978; 283:53–77. [PubMed: 722589]
- Newman LA, Korol DL, Gold PE. Lactate produced by glycogenolysis in astrocytes regulates memory processing. *PLoS One*. 2011; 6:e28427. [PubMed: 22180782]
- Pellerin L, Magistretti PJ. Glutamate uptake into astrocytes stimulates aerobic glycolysis: a mechanism coupling neuronal activity to glucose utilization. *Proceedings of the National Academy of Sciences of the United States of America*. 1994; 91:10625–10629. [PubMed: 7938003]
- Pellerin L, Pellegri G, Bittar PG, Charnay Y, Bouras C, Martin JL, Stella N, Magistretti PJ. Evidence supporting the existence of an activity-dependent astrocyte-neuron lactate shuttle. *Developmental Neuroscience*. 1998; 20:291–299. [PubMed: 9778565]
- Poitry-Yamate CL, Poitry S, Tsacopoulos M. Lactate released by Muller glial cells is metabolized by photoreceptors from mammalian retina. *The Journal of Neuroscience*. 1995; 15:5179–5191. [PubMed: 7623144]
- Prichard J, Rothman D, Novotny E, Petroff O, Kuwabara T, Avison M, Howseman A, Hanstock C, Shulman R. Lactate rise detected by 1H NMR in human visual cortex during physiologic

- stimulation. Proceedings of the National Academy of Sciences of the United States of America. 1991; 88:5829–5831. [PubMed: 2062861]
- Ros J, Jones D, Pecinska N, Alessandri B, Boutelle M, Landolt H, Fillenz M. Glutamate infusion coupled with hypoxia has a neuroprotective effect in the rat. *J Neurosci Methods*. 2002; 119:129–133. [PubMed: 12323416]
- Sampol D, Ostrofet E, Jobin ML, Raffard G, Sanchez S, Bouchaud V, Franconi JM, Bonvento G, Bouzier-Sore AK. Glucose and lactate metabolism in the awake and stimulated rat: a (13)C-NMR study. *Frontiers in Neuroenergetics*. 2013; 5:5. [PubMed: 23755012]
- Schurr A, Payne RS, Miller JJ, Rigor BM. Brain lactate, not glucose, fuels the recovery of synaptic function from hypoxia upon reoxygenation: an in vitro study. *Brain Res*. 1997; 744:105–111. [PubMed: 9030418]
- Siesjo, BK. *Brain Energy Metabolism*. John Wiley & Sons; New York: 1978.
- Smith D, Pernet A, Hallett WA, Bingham E, Marsden PK, Amiel SA. Lactate: a preferred fuel for human brain metabolism in vivo. *Journal of Cerebral Blood Flow & Metabolism*. 2003; 23:658–664. [PubMed: 12796713]
- Sokoloff L. The brain as a chemical machine. *Progress in Brain Research*. 1992; 94:19–33. [PubMed: 1337612]
- Swanson RA, Morton MM, Sagar SM, Sharp FR. Sensory stimulation induces local cerebral glycogenolysis: demonstration by autoradiography. *Neuroscience*. 1992; 51:451–461. [PubMed: 1465204]
- Thomson D. Spectrum estimation and harmonic analysis. *Proc IEEE*. 1982; 70:1055–1096.
- Vlassenko AG, Rundle MM, Mintun MA. Human brain glucose metabolism may evolve during activation: findings from a modified FDG PET paradigm. *Neuroimage*. 2006; 33:1036–1041. [PubMed: 17035047]
- Wilson GS, Zhang Y, Reach G, Moatti-Sirat D, Poitout V, Thevenot DR, Lemonnier F, Klein JC. Progress toward the development of an implantable sensor for glucose. *Clin Chem*. 1992; 38:1613–1617. [PubMed: 1525989]
- Wyss MT, Jolivet R, Buck A, Magistretti PJ, Weber B. In vivo evidence for lactate as a neuronal energy source. *The Journal of Neuroscience*. 2011; 31:7477–7485. [PubMed: 21593331]
- Xing D, Yeh CI, Burns S, Shapley RM. Laminar analysis of visually evoked activity in the primary visual cortex. *Proc Natl Acad Sci U S A*. 2012; 109:13871–13876. [PubMed: 22872866]
- Yanai S, Nisimaru N, Soeda T, Yamada K. Simultaneous measurements of lactate and blood flow during hypoxia and recovery from hypoxia in a localized region in the brain of the anesthetized rabbit. *Neurosci Res*. 1997; 27:75–84. [PubMed: 9089701]

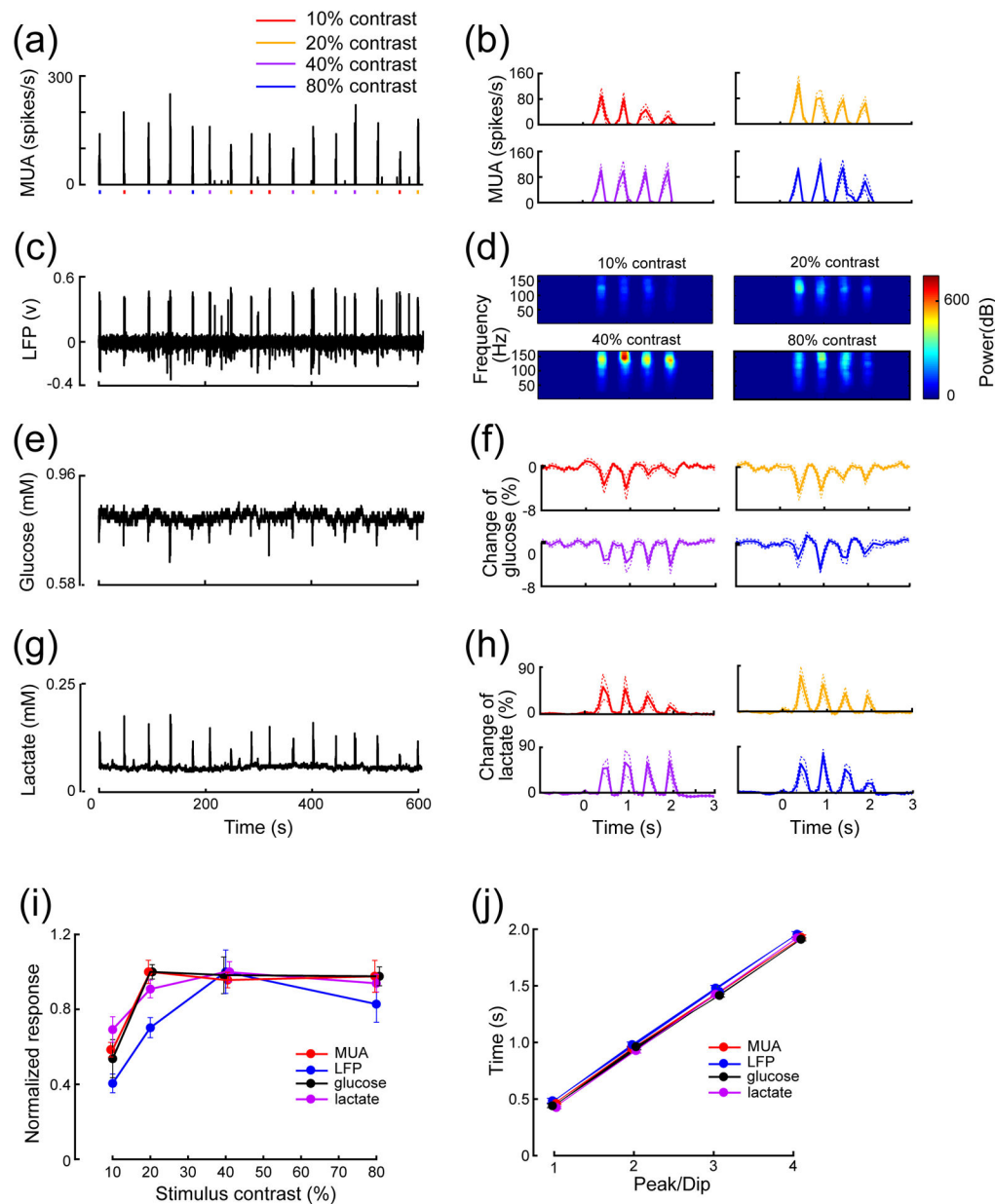


**Fig. 1.** Simultaneous measurements of neural and metabolic responses for a recording site in the visual cortex. (a–d) Multiple unit activity (MUA), local field potential (LFP), glucose, and lactate responses to repetitive visual stimuli of different contrast levels (10%, 20%, 40%, and 80%). Horizontal short bars of different colors represent stimulus onset and duration (30 s), and data include eight trials for each contrast level (left column). The temporal and spatial frequencies are 2 Hz and 0.12 cycles/deg. respectively. The stimulus size is 8 deg. in diameter. The depth of this recording site is 4030  $\mu\text{m}$  from the cortical surface. To compare the coupling between neural and metabolic responses, neural activity is grouped at a bin size of 100 ms to match the sampling rate of 10 Hz for glucose and lactate signals. Data within the two black vertical dashed lines (left column) are zoomed in on and displayed in middle column. The orange horizontal bar (a, middle column) represents stimulus onset and duration (30 s). To visualize the detailed dynamic changes over time, data within the two red vertical dashed lines in the middle column are zoomed in on and shown in the right column. The LFP spectrums are shown as modulated signal power (dB) as a function of frequency and time (b, insets, middle and right columns). (e–g) Distribution of time differences between neural peak and glucose dip (e), neural and lactate peaks (f) and glucose dip and lactate peak (g).



**Fig. 2.** Average neural, glucose and lactate responses to visual stimuli. Data are averaged across 16 trials. The duration of visual stimuli is 30 s. (a–c) Neural, glucose and lactate responses have a temporal resolution of 10 Hz. (d–f) Data in a–c are averaged across every 5 data points and re-plotted here. The temporal resolution is 2 Hz. (g) Contrast tuning functions for neural, glucose, and lactate responses for the four contrast levels. A tight coupling is shown here between the three measurements. (h) Percent changes of glucose and lactate signals as a function of spiking rate. Absolute values are shown for changes in glucose responses (g, h). Dotted lines and error bars stand for s.e.m.



**Fig. 3.**

A short-duration stimulus elicited significant responses. (a, c, e, g) MUA, LFP, glucose, and lactate responses to visual stimuli of different contrast levels. The colored short bars represent stimulus onsets and duration (2 s). The temporal and spatial frequencies are 2 Hz and 1.07 cycles/deg. respectively. The stimulus size is 5 deg. in diameter. The depth of this recording site is 876  $\mu\text{m}$  from cortical surface. (b, d, f, h) Averaged responses across multiple trials for MUA, LFP, glucose, and lactate. Curves of different colors represent responses to different contrast levels. (i) Normalized MUA, LFP, glucose and lactate responses to visual stimuli at different contrast levels. (j) Comparison of average times for the 4 peaks (dips) across multiple trials ( $n=8$ ). Dotted lines stand for s.e.m.

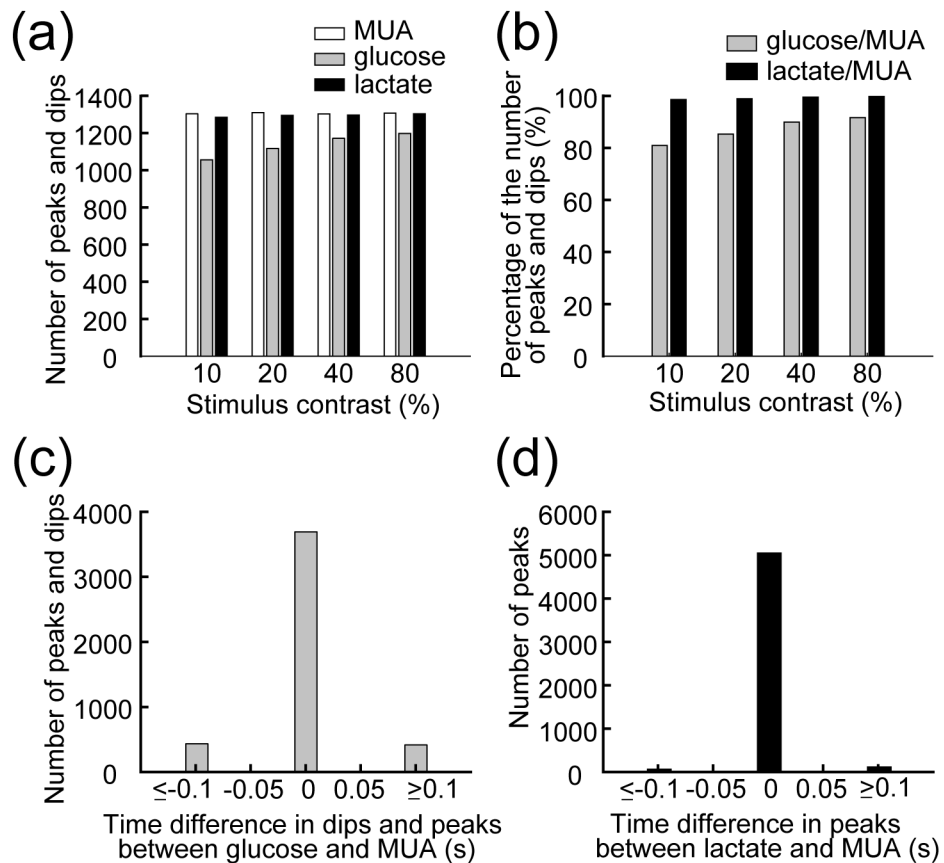


**Fig. 4.** Tight coupling in time between neural, glucose, and lactate responses across a population of recording sites. (a) Comparison of numbers of peaks or dips for MUA, glucose, and lactate responses. (b) Comparison of percentages of glucose dips and lactate peaks normalized by the numbers of MUA peaks. (c–d) Distribution of time differences between glucose dips and corresponding MUA peaks (c) and between lactate peaks and corresponding MUA peaks (d), respectively.

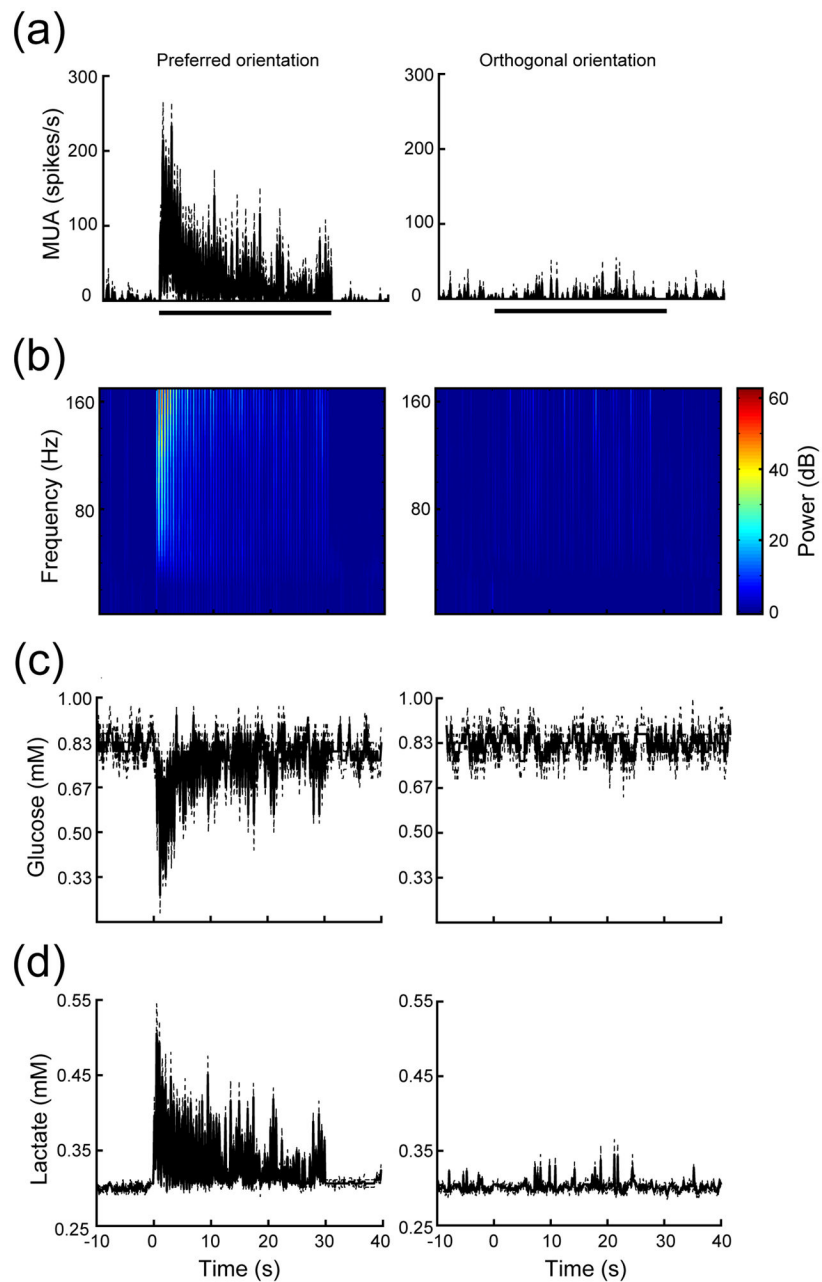


**Fig. 5.** Orientation selectivity of neural, glucose, and lactate responses to visual stimuli. The stimulus at preferred orientation (a–d, left column) elicited vigorous MUA (a), LFP (b), glucose (c) and lactate (d) responses compared to that at an orthogonal orientation (a–d, right column). The preferred orientation is  $245^\circ$ , and the orthogonal orientation is  $335^\circ$ . The stimulus contrast level is 50%. The temporal and spatial frequencies are 2 Hz and 0.12 cycles/deg., respectively. The depth of this recording site is  $4601 \mu\text{m}$ . Horizontal bars in (a) represent stimulus onset and duration (30 s). Dotted lines represent s.e.m.

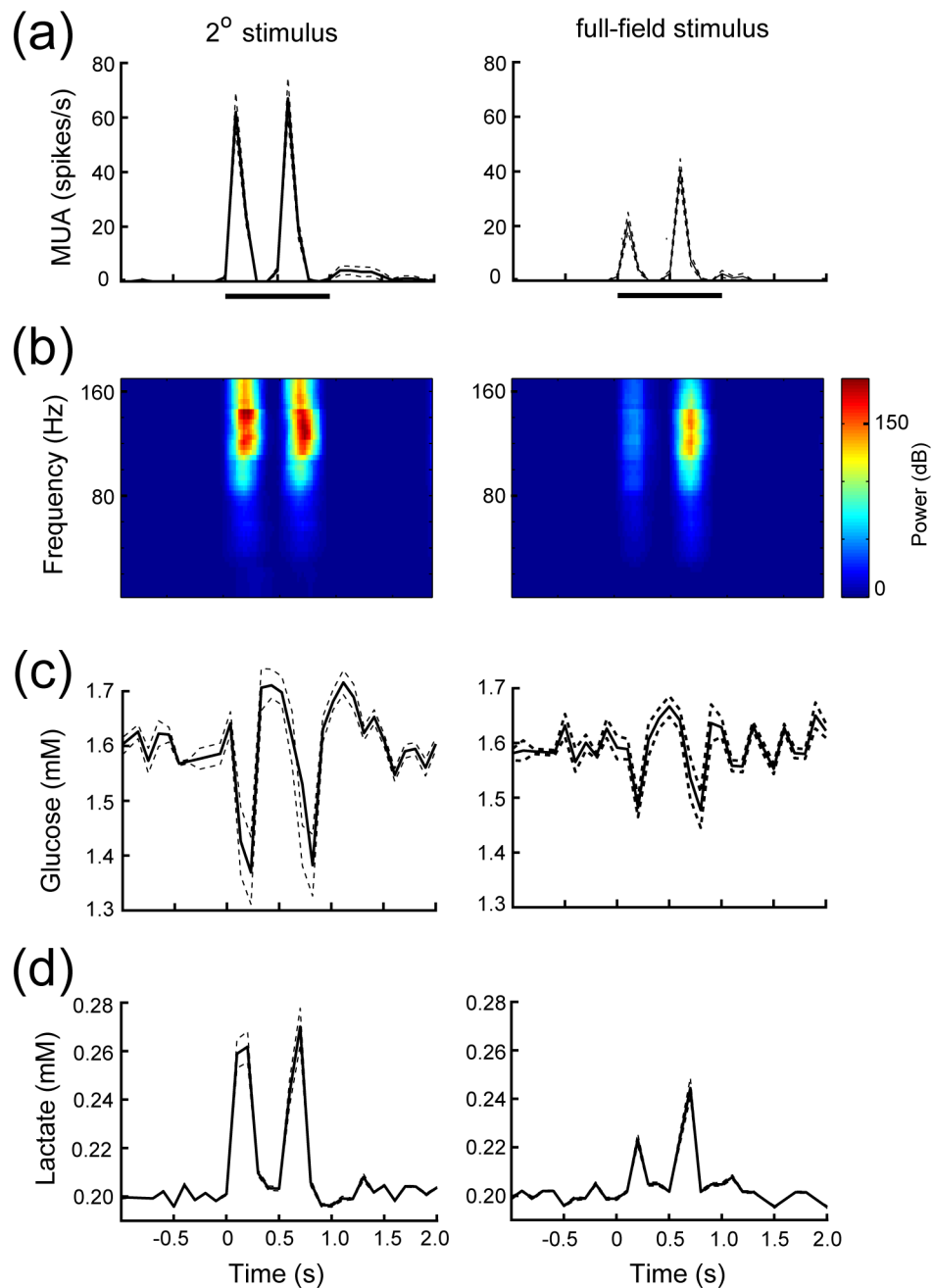


**Fig. 6.** Neural, glucose, and lactate responses to visual stimuli of different sizes. The 2° stimulus (a–d, left column) is the optimal size which elicits maximum firing rate of neural responses. The full-field stimulus (a–d, right column) is 66° × 37° which is the maximum size of visual stimulus in the experiment. Stimulus duration is 1 s. Horizontal bars represent stimulus onset and duration. The temporal and spatial frequencies are 2 Hz and 0.5 cycles/deg., respectively. The stimulus contrast is 50%. The depth of this recording site is 1726  $\mu\text{m}$ . Note that all measurements are modulated at the temporal frequency (2 Hz) for visual stimuli at different sizes.

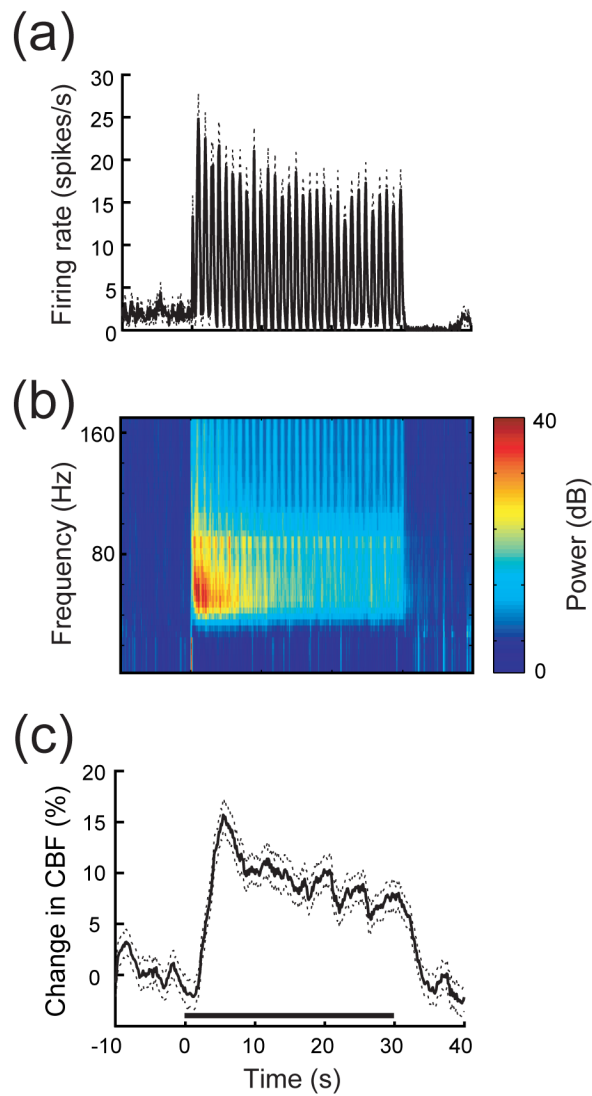


**Fig. 7.** Simultaneous measurements of cerebral blood flow (CBF) and neural activity to visual stimulus. Both MUA (a) and LFP (b) exhibit a simple-cell pattern that is modulated in synchrony with the temporal frequency of stimulation. However, the CBF signal shows a sustained high-level change during visual stimulation (c). The stimulus size is  $2^\circ$  in diameter. The temporal and spatial frequencies are 1 Hz and 0.52 cycles/deg., respectively. The depth of this recording site is 1534  $\mu\text{m}$ . The horizontal bar represents stimulus onset and duration (30 s). Dotted lines represent s.e.m.